International Journal of Basic and Applied Sciences, 14 (SI-2) (2025) 183-188

International Journal of Basic and Applied Sciences

Website: www.sciencepubco.com/index.php/IJBAS
https://doi.org/10.14419/wt674v75
Research paper

Experimental Study of Dross Height Formation for CO_2 and Fiber Laser Machining of SS 310 Material

Sachin Malave [1]*, Aniket Jadhav [2], Nitish Kumar Gautam[3]

[1] Research Scholar, Department of Mechanical Engineering, Shri Jagdishprasad Jhabarmal Tibrewala University, Vidyanagri, Jhunjhunu-333010, Rajasthan, India
[2] Assistant Professor, Department of Mechanical Engineering, Smt. Kashibai Navale College of Engineering, Pune-411041, Maharashtra, India
[3] Assistant Professor, Department of Mechanical Engineering, Shri Jagdishprasad Jhabarmal Tibrewala University, Vidyanagri, Jhunjhunu-333010, Rajasthan, India
**Corresponding author E-mail:skmalave.scoe@gmail.com*

Received: June 15, 2025, Accepted: August 1, 2025, Published: August 12, 2025

Abstract

Laser cutting is a popular non-traditional thermal machining technique. With this machining technique, almost all the materials having com-plex geometries are machined with higher accuracy. In this paper experimental study of dross height formation on 25 mm thick laser machining of SS 310 material utilizing CO_2 laser and fiber lasers is carried out. Dross height is measured to evaluate the influence of varying process parameters, consisting of gas pressure, cutting speed, and laser power. For the experimental task, a Bystronic laser machine is utilized. There are 17 trial runs in all, with three components and two levels selected. ANOVA is utilized in mathematical calculations. The optimized values during laser machining are identified for the process parameters. Optimum values for these factors are defined with the goal of attaining the minimum dross height. The primary interpretation made from this experimental study is that dross height increases as there is increase in the laser power.

Keywords*: laser machining, optimization, dross height formation, DOE, laser power*

1. Introduction

Nowadays industrialists are facing intense competition due to changing market scenario. It has resulted in customers demanding higher quality goods at lower prices. Manufacturers are trying to supply the goods as per the customer's expectations, that matches so that the quality is provided. Laser processing of the goods offers significant advantages over the other non-conventional manufacturing methods. It has many advantages compared to other traditional manufacturing methods [5]. Laser beam machine (LBM) is two-dimensional machining method. It is used to remove the material by focusing the beam of laser on surface of a workpiece. In industries, LBM has wide range of applications. Normally there are two forms of laser process used for cutting metal: CO_2 and fiber lasers. Each type has benefits and drawbacks. Out of these two types which is better is not yet understood. Therefore, an experimental investigation of both laser types is attempted in this research work. SS 310 material is an austenitic steel. It has higher corrosion resistance and good mechanical properties. This material is mainly used in chemical industries and automotive sectors due to high heat-resistant properties [30]. Dross formation is the material that solidifies along the lower edge of the substrate during laser cutting and looks as solidified material as shown in dross height formation setup diagram (Fig. 1). Dross formation depends on the viscosity of the liquid material. Dross occurs in materials having high surface tension. As the surface tension of metals is normally higher than that of oxides, gas pressure produces drops height formation [4].

Alsaadawy et al. [2] studied LBM on a thick sheet, optimizing power, velocity, and gas pressure of cutting quality. The optimal kerf width, surface roughness, dross height formation and kerf taper angle were achieved under varying conditions of laser parameters. Eaysin et al. [7] utilized a fiber laser beam machining for the accurate cutting of steel material. The experiments were designed using the Taguchi 27 model. The study concentrated on the kerf characteristics and surface roughness as response variables. Ji et al. [14] predicted kerf width and dross formation during laser machining of an alloy. The model incorporated few machining parameters such as feed rate, standoff distance, duty cycle, etc. Okamoto et al. [21] concluded that fiber machining of a steel plate using a twin-spot beam configuration aligned with the scanning direction effectively reduces dross height by controlling heat input to different parts of the specimen. Bach et al. [6] investigated the stimulus of dross formation on AISI 304 using iterative experimental design, and four distinct dross geometries were studied to categorize the manufacturing parameters related to dross height formations. Kardan et al. [16] explored the effects of dynamic beam shaping parameters on dross, indicating that optimal amplitude and frequency settings significantly reduces dross height during laser cutting of thick plates. Mahrle et al. [18] examined the issue of varying liability for the dross and differences in the performance of LBM of steel material. Sargar et al. [27] analyzed the effect of input variables on dross formation during CO_2 and fiber laser cutting on steel material.

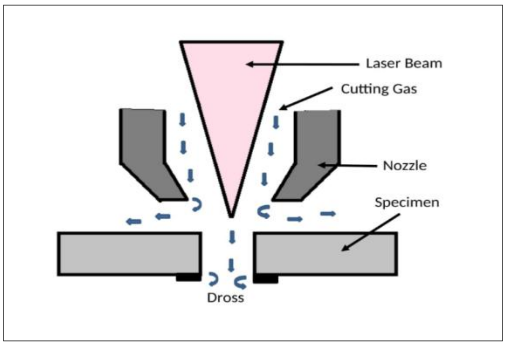

Fig. 1: Dross height formation setup diagram

The study focused on the experimental analysis of laser beam cutting for 20 mm thick steel material. The findings revealed that the CO_2 laser machining produced superior machining effect than the fiber laser process. A key conclusion from the study was that cutting speed significantly impacts dross height, while gas pressure showed minimal effect on dross height formation. Mathematical models were developed to forecast machining performance, while the influence of the power of laser, frequency, speed and nozzle tip distance were systematically analyzed by Rao et al. [25]. Rohman et al. [26] performed artificial neural network and grey wolf optimizer to study the input process parameters for minimum dross height formation. Nabavi et al. [20] developed model for dross height during cutting using energy and gas-based parameters. Validation through fiber cutting of stainless steel revealed that gas-based parameters significantly affect dross diameter, with the model showing improved accuracy over previous studies. Alsoruji et al. [3] studied on laser drilling of Nickel alloy using Taguchi method to enhance machining performance. Optimal process factors were identified, achieving a very low accuracy improvement. Gas pressure was found to dominate performance measures, ensuring concentrated energy and better surface topography with minimal microcracks. Kai et al. [15] investigated that the beam intensity distribution significantly affects dross height. Specifically, using a square top-hat mode results in smaller dross height compared to a round Gaussian mode, due to increased energy uniformity on the cutting surface. Singh et al. [28] discussed that laser machining parameters significantly influence dross height in Titanium alloy cutting. Optimizing parameters such as power, speed, and pressure can effectively reduce dross during the cutting. The machinability of composite materials, which are frequently utilized in industries, was examined by Abedinzadeh et al. [1]. Laser assisted cutting was completed on samples fabricated using electromagnetic stir casting and analyzed through Taguchi standard orthogonal method (L9). Optimal conditions for roughness using power, speed, depth of cut was identified. Jadhav and Kumar [13] conducted an experimental study the influence input variables on dross height obtained by LBM of AISI 304 material. Additionally, a mathematical equation was created to analyze the dross height. Yagi et al. [31] examined how the angle alignment between the nozzle and laser power center affects cutting quality using computational fluid dynamics analysis method. Franceschetti et al. [8] found that speed, power and pressure significantly influence dross attachment. Variations in these parameters leads to increased dross levels. Hu et al. [12] investigated that the cutting speed and defocusing amount significantly influence dross formation during laser cutting. Higher cutting speeds and optimal defocus settings reduces dross height, improving overall cutting quality in stainless steel sheets. Patel and Bhavsar [22] investigated the consequence of LBM constraints on dross, indicating that variations in constraints such as feed rate, power, and pulse duration impacting dross formation during LBM. Patel and Bhavsar [23] investigated how laser machining parameters (speed, power, and assist gas pressure), influence dross height for alloy steel. Optimizing these parameters minimizes dross formation, enhancing the quality of the cut and overall machining efficiency. Hiwale and Rajiv [11] concluded the impact of laser process variables such as power, pressure, etc. on characteristics of the top and bottom kerf formation. Muthuramalingam et al. [19] examined the influence of input variables during LBM of alloy steel. Parameters were evaluated for their influence on dimensional accuracy measures like roundness and ovality. Power is the important parameter with the optimal parameter combination of gas pressure and laser power. Garcia-Lopez et al. [9] found that back wall dross height ranged from 0.24% to 0.94% under normal conditions, achieved by blowing argon gas, indicating significant influence on dross behavior. Garcia-Lopez et al. [10] identified the influence of fiber laser process for surface roughness and the dross formation of AISI 316 L material. They focused on investigating laser process parameters (peak power, machining speed and gas pressure). Petkovic et al. [24] investigated the heat affected zone in laser processes by analyzing the stimulus of power, speed and pressure using the artificial neural network. Cutting speed is found to have highest impact, while gas pressure had the least influence. Leone et al. [17] explored LBM on aluminum alloy sheets using Nd:YAG laser. The results demonstrate the capability to cut 1 mm sheets at lower dross height. Teixidor et al. [29] studied that the influence of process variables for dross height during fiber machining of 316 L material. Optimizing process variable effectively minimizes dross, improving cutting quality and precision.

2. Experimental Work

All the experimental work is performed on CO_2 and fiber laser beam machine available at M/s Kakade lasers, Narhe, Pune, India. Specifications of CO_2 and fiber LBM setup are given in Table 1.

Table 1: Specifications of CO_2 and fiber LBM setup

	CO_2 laser Machine	Fiber Laser Machine
Composition	CO_2+He+N2	1% Nd doped Yttrium-Aluminium-Garnet
Emission wave length	10.64 μm	1.064 μm
Efficiency	12-16 %	3 %
Spot size	0.080 mm	0.020 mm
Peak power	12 kW	12 kW
Work table	6000 × 2800 mm	6000 × 2500 mm
Nozzle diameter	4 mm	3 mm

For the present experimental work, SS 310 material is used. It has yield strength of 205 MPa, tensile strength of 517 MPa and modulus of elasticity is around 200 GPa. Plates (size: 350 mm× 450 mm) of thicknesses 25 mm are purchased from M/s Mahalaxmi Material Store, Narhe, Pune, India. The chemical content of SS 310 material is stated in the Table 2.

Table 2: Chemical content of SS 310 material

C	Cr	Ni	Si	Mn	P	S	Fe
0.24	23.0 – 25.0	18.1 – 23.0	1.50	2.10	0.055	0.04	Balance

After experimental work, the dross formation at the lower part of the specimen is measured by taking images of the machined surfaces using Digital Single Lens Reflex (DSLE) camera. Then these images are transferred to the desktop screen and the dross height formation is measured using "Image J" software. This software is used as it provides higher accuracy in terms of measurement.

3. Results and Discussions

Table 3. lists the calculated values for dross height of machined specimens of thickness 25 mm by CO_2 and fiber laser. In order to avoid repeatability each experimental run was repeated three times for ensuring consistency.

Table 3: Dross height of machined specimens of thickness 25 mm

	Process parameters			Dross height (mm)	
S. No.	**A (watt)**	**B (mm/min)**	**C (bar)**	**CO_2 laser**	**Fiber laser**
1	5500	175	12	2.7	2.4
2	5750	175	10	2.85	2.5
3	5750	175	10	2.85	2.5
4	5500	150	10	2.45	2.25
5	5750	175	10	3.1	2.6
6	5500	175	8	3.25	2.3
7	6000	175	12	2.75	2.45
8	5750	175	10	2.95	2.55
9	6000	200	10	3	2.35
10	6000	150	10	2.5	2.3
11	5750	200	8	4	3.5
12	5750	150	8	2.65	3.35
13	5750	200	12	3.5	3.2
14	5750	150	12	2.25	2.2
15	5750	175	10	3	2.55
16	6000	175	8	2.85	2.75
17	5500	200	10	3.85	3.3

were, A – laser power, B - cutting speed, C – gas pressure
ANOVA for dross height of specimens of thickness 25 mm machined by CO_2 laser is given in Table 4.

Table 4: ANOVA for dross height of specimens of thickness 25 mm machined by CO_2 laser

Source	SS	MS	F-value	p-value	
Model	3.35	0.3723	18.70	0.0004	significant
A	0.1653	0.1653	8.30	0.0236	
B	2.53	2.53	127.13	< 0.0001	
C	0.3003	0.3003	15.08	0.0060	
AB	0.2025	0.2025	10.17	0.0153	
AC	0.0506	0.0506	2.54	0.1548	
BC	0.0025	0.0025	0.1256	0.7335	
A^2	0.0475	0.0475	2.39	0.1662	
B^2	0.0475	0.0475	2.39	0.1662	
C^2	0.0081	0.0081	0.4048	0.5449	
Residual	0.1394	0.0199			
LF	0.0944	0.0315	2.80	0.1730	not significant
PE	0.0450	0.0113			
Cor Total	3.49				

where, SS – sum of squares, MS – mean square, LF – lack of fit, PE – pure error
For CO_2 laser machining, models are significant with F-value of 18.70. It is identified that gas pressure, power and cutting speed are important terms. It is also noticed that the interactions of power and speed show similar effects. The F-value of 2.80 represents lack of fit is not significant. The Predicted R-squared (0.8472) is in reasonable agreement with the Adjusted R-squared (0.9087). Predictive model for dross height in terms of coded factors gives Equation (1) based on the analysis.

$$\text{Dross height} = 2.95 - 0.14375 \times A + 0.5625 \times B - 0.19375 \times C - 0.225 \times AB + 0.1125 \times AC - 0.025 \times BC - 0.10625 \times A^2 + 0.10625 \times B^2 + 0.04375 \times C^2 \quad (1)$$

Equation (2) state predictive model for the dross height in terms of actual factors.

$$\text{Dross height} = - 70.7812 + 0.023025 \times A + 0.175 \times B - 1.52187 - 3.6 \times 10\text{-}5 \times AB + 0.000225 \times AC - 0.0005 \times BC - 1.710\text{-}6 \times A^2 + 0.00017 \times B^2 + 0.0109375 \times C^2 \quad (2)$$

The ANOVA for dross height of specimens for fiber laser is given in Table 5.

Table 5: ANOVA for dross height of specimens of thickness 25 mm machined by fiber laser

Source	SS	MS	F-value	p-value	
Model	2.78	0.3089	61.56	< 0.0001	significant
A	0.0450	0.0450	8.97	0.0201	
B	2.26	2.26	449.96	< 0.0001	
C	0.0528	0.0528	10.52	0.0142	
AB	0.0000	0.0000	0.0000	1.0000	
AC	0.0400	0.0400	7.97	0.0256	
BC	0.0056	0.0056	1.12	0.3249	
A²	0.0063	0.0063	1.26	0.2987	
B²	0.3758	0.3758	74.89	< 0.0001	
C²	0.0029	0.0029	0.5782	0.4718	
Residual	0.0351	0.0050			
LF	0.0281	0.0094	5.36	0.0693	not significant
PE	0.0070	0.0017			
Cor Total	2.82				

As per the ANOVA results, the model is significant for fiber laser machining with F-value of 61.56. It is observed that laser power, speed and gas pressure are the important terms. It is also found that interaction of gas pressure and laser power are significant. F-value of 5.36 represents non-significant terms. The Predicted R-squared of 0.8363 is in reasonable agreement with the Adjusted R-squared of 0.9715. Equation (3) and Equation (4) give the predictive model for dross height formation for coded and actual factors respectively.

$$\text{Dross height} = 2.54 + 0.075 \times A + 0.53125 \times B - 0.08125 \times C - 6.1917310\text{-}16 \times AB - 0.1 \times AC - 0.0375 \times BC - 0.03875 \times A^2 + 0.29875 \times B^2 - 0.02625 \times C^2 \quad (3)$$

$$\text{Dross height} = -21.8262 + 0.00943 \times A - 0.13855 \times B + 1.37187 \times C + 2.1299110\text{-}18 \times AB - 0.0002 \times AC - 0.00075 \times BC - 6.210\text{-}7 \times A^2 + 0.000478 \times B^2 - 0.0065625 \times C^2 \quad (4)$$

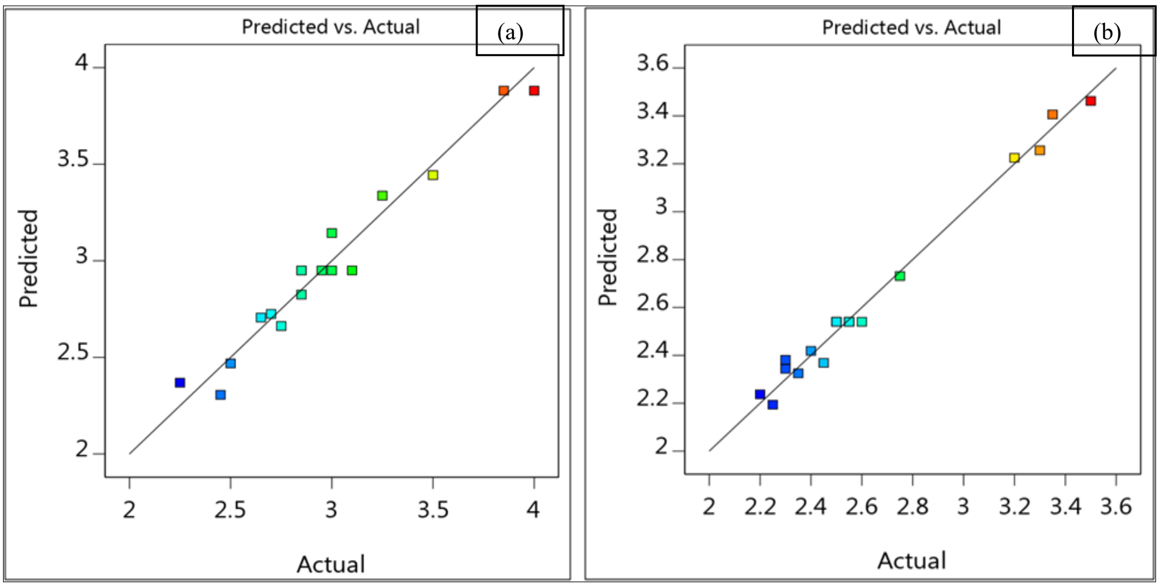

Fig. 2: Predicted v/s actual values for dross height of specimen thickness 25 mm (a) CO_2 laser and (b) fiber laser

Fig. 2. (a) and (b) show predicted v/s actual values for dross height of specimen thickness 25 mm by CO_2 and fiber laser respectively. It is found that the model predictions and the experimental results are in alignment with each other. The influence of process values for dross height of specimen thickness 25 mm by CO_2 and fiber laser is shown in Fig. 3. (a) and (b). It is found that as power and gas pressure decrease there is small enhancement in dross height. Lower power causes incomplete cutting causing dross formation and rough edges. Dross height increases with the increase in cutting speed. Due to the higher cutting speed there is not enough time for the material to completely eject from the lower part and leads to the formation of dross. These results follow the same trends as observed for SS 310 material for lower thickness also. From the above experimental work, it is found that the dross height formation is less in case of CO_2 laser as compared to fiber for laser machining of SS 310 material. Table 6. lists the minimum and maximum response characteristic values of specimen machined by CO_2 and fiber laser. Therefore, for laser process of SS 310 material of thickness 25 mm, CO_2 laser is preferred as compared to fiber laser. It is also observed that sometimes non-uniform trend of effect of process values on the response characteristics is found for fiber laser process. The wavelength of light emitted by CO_2 laser (typically 10.64 um) is higher than the fiber laser, with a high beam focal diameter which offers higher heating of the material as compared to fiber laser technology. Also, in this machinery no gas consumables are used. Fiber laser machine produces less vapour pressure to blow away the melt material. The more localized heat of fiber lasers creates thicker melt pools and are harder to eject resulting in higher dross formation.

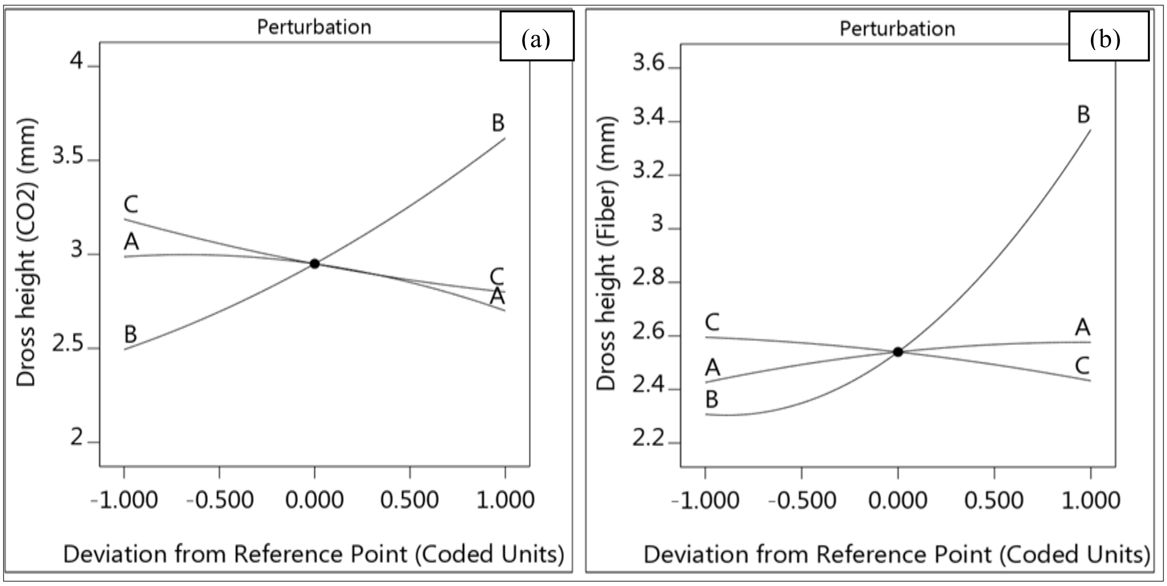

Fig. 3: Influence of process parameter for dross height of specimen thickness 25 mm, (a) CO_2 laser and (b) fiber laser

Table 6: Minimum and maximum response characteristic values of machined specimen by CO_2 and fiber laser

	25 mm	
Response characteristic	Minimum	Maximum
Dross height (CO_2)	1.5	3.5
Dross height (fiber)	0.75	2.35

Table 7. lists the optimization criteria for dross height of machined specimen of thickness 25 mm by CO_2 and fiber laser. It is found that the optimum value for dross height by CO_2 and fiber LBM is 3.478 and 3.125 respectively. The optimized parameters are justified as optimal as they represent the most feasible compromise within the defined process window. It offers predictable and balanced performance rather than only pursuing the lowest recorded dross height formation.

Table 7: Optimization criteria for dross height of machined specimen of thickness 25 mm

Name	**LL**	**UL**	**OV**
A	5500	6000	5758.789
B	150	200	187.487
C	8	12	12.478
Dross height for CO_2 laser (mm)	2.65	5	3.478
Dross height for fiber laser (mm)	2.1	2.5	3.125

where, LL – lower limit, UL – upper limit, OV – optimized value

Bar graph of desirability for dross height of specimens of thickness 25 mm machined by CO_2 and fiber laser is shown in Fig. 4. Desirability value for dross height of all process parameters, CO_2 laser, fiber laser and combined influence is 1 and therefore acceptable.

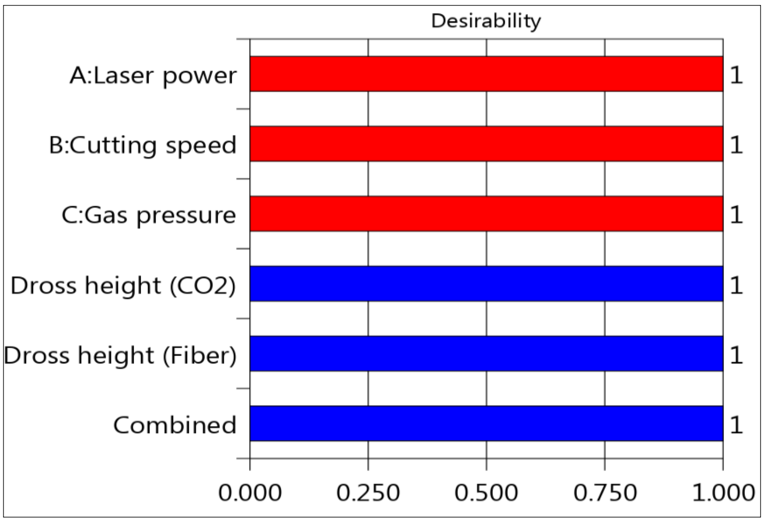

Fig. 4: Bar graph of desirability for dross height of specimens of thickness 25 mm machined by CO_2 and fiber laser

4. Conclusion

In the present experimental study, an investigation of influence of the input parameters for CO_2 laser and fiber laser machining on SS 310 material is conducted. After design of experiment analysis 17 experimental runs were recognized for trials. A quality-driven analysis and optimization is conducted applying response surface methodology by utilizing Box Behnken design to obtain the anticipated cut quality.

The ideal settings of these factors are characterized by attaining the least dross height. For SS 310 material cutting speed is the most important parameter in comparison with the gas pressure and laser power. An increase in cutting speed causes corresponding rise in dross height. Power of laser and gas pressure did not have significant influence on the change in dross height.

References

[1] Abedinzadeh, R., Norouzi, E., and Toghraie, D. (2021) Experimental investigation of machinability in laser-assisted machining of aluminum-based nanocomposites. Journal of Materials Research and Technology, 15, 3481–3491.

[2] Alsaadawy, M., Dewidar, M., Said, A., Maher, I., and Shehabeldeen, T. A. (2024) Investigation of the effect of laser cutting parameters on surface and kerf quality of thick TI–6AL–4V alloy sheets. Arabian Journal for Science and Engineering.

[3] Alsoruji, G., Muthuramalingam, T., Moustafa, E. B., and Elsheikh, A. (2022) Investigation and TGRA based optimization of laser beam drilling process during machining of Nickel Inconel 718 alloy. Journal of Materials Research and Technology, 18, 720–730.

[4] Jadhav, A., and Kumar, S. (2019) An experimental study of influence of process parameters on dross properties in laser machining of AISI 304 material. Journal of Manufacturing Engineering, 111–116.

[5] Jadhav, A., and Kumar, S. (2019) Laser cutting of AISI 304 material: an experimental investigation on surface roughness. Advances in Materials and Processing Technologies, 429–437.

[6] Bach, J., Zeuner, A. T., Wanski, T., Fischer, S. C. L., Herwig, P., and Zimmermann, M. (2023) Influence of the dross formation of the laser-cut edge on the fatigue strength of AISI 304. Metals, 13 (3), 624.

[7] Eaysin, A., Kabir, S., Gunister, E., Jahan, N., Hamza, A., Zinnah, M. A., and Rashid, A. B. (2024) Process parameter optimization of laser beam machining for AISI-P20 mold steel using ANFIS method. Results in Surfaces and Interfaces, 100357.

[8] Franceschetti, L., Pacher, M., Tanelli, M., Strada, S. C., Previtali, B., and Savaresi, S. M. (2022) Dross attachment estimation in the laser-cutting process via convolutional neural networks (CNN). In 30th Mediterranean Conference on Control and Automation (MED), 850–855.

[9] Garcia-Lopez, E., Ibarra-Medina, J. R., Siller, H. R., Lammel-Lindemann, J. A., and Rodriguez, C. A. (2018) Surface finish and back-wall dross behavior during the fiber laser cutting of AZ31 magnesium alloy. Micromachines, 9 (10), 485.

[10] Garcia-Lopez, E., Medrano-Tellez, A., Ibarra-Medina, J., Siller, H., and Rodriguez, C. (2017) Experimental study of back wall dross and surface roughness in fiber laser microcutting of 316L miniature tubes. Micromachines, 9 (1), 4.

[11] Hiwale, S., and Rajiv, B. (2020) Experimental investigations of laser machining process parameters using response surface methodology. Materials Today: Proceedings, 44, 3939–3945.

[12] Hu, C., Mi, G., and Wang, C. (2020) Study on surface morphology and recast layer microstructure of medium thickness stainless steel sheets using high power laser cutting. Journal of Laser Applications, 32 (2).

[13] Jadhav, A., and Kumar, S. (2020) Laser machining of AISI 304: an experimental study of influence of process parameters on dross height formation. In Lecture Notes in Mechanical Engineering, 537–545.

[14] Ji, M., Thangaraj, M., Devaraj, S., Machnik, R., Karkalos, N. E., and Karmiris-Obratański, P. (2024) Prediction and optimization kerf width in laser beam machining of titanium alloy using genetic algorithm tuned adaptive neuro-fuzzy inference system. The International Journal of Advanced Manufacturing Technology, 132 (11–12), 5873–589.

[15] Kai, N., Okamoto, Y., Okada, A., Ishiguro, H., Ito, R., Sugiyama, A., Okawa, H., and Fujita, R. (2021) Investigation on reduction of dross height by analyzing beam intensity distribution in fiber laser cutting. Journal of Laser Applications, 33 (4).

[16] Kardan, M., Levichev, N., Castagne, S., and Duflou, J. R. (2023) Dynamic beam shaping requirements for fiber laser cutting of thick plates. Journal of Manufacturing Processes, 103, 287–297.

[17] Leone, C., Genna, S., Caggiano, A., Tagliaferri, V., and Molitierno, R. (2015) An investigation on ND:YAG laser cutting of AL 6061 T6 alloy sheet. Procedia CIRP, 28, 64–69.

[18] Mahrle, A., Wanski, T., Zeuner, A. T., Herwig, P., and Zimmermann, M. (2023) Investigations on dross formation susceptibility in laser fusion cutting of different stainless-steel compositions with emphasis on minor element effects. Journal of Laser Applications, 35 (3).

[19] Muthuramalingam, T., Moiduddin, K., Akash, R., Krishnan, S., Mian, S. H., Ameen, W., and Alkhalefah, H. (2020) Influence of process parameters on dimensional accuracy of machined Titanium (Ti-6Al-4V) alloy in laser beam machining process. Optics and Laser Technology, 132, 106494.

[20] Nabavi, S. F., Farshidianfar, M. H., Farshidianfar, A., and Marandi, S. (2022) Dross formation modeling in the laser beam cutting process using energy-based and gas-based parameters. The International Journal of Advanced Manufacturing Technology, 120 (11–12), 8169–8184.

[21] Okamoto, Y., Morimoto, K., Kai, N., Okada, A., Ishiguro, H., Ito, R., and Okawa, H. (2023) Fiber laser cutting of steel plate by twin spot beam setting in scanning direction. Journal of Laser Applications, 35 (4).

[22] Patel, A. R., and Bhavsar, S. N. (2020) Laser machining of die steel (En-31): an experimental investigation to study the effect of process parameters. Advances in Materials and Processing Technologies, 8 (1), 688–702.

[23] Patel, A., and Bhavsar, S. N. (2020) Experimental investigation to optimize laser cutting process parameters for difficult to cut die alloy steel using response surface methodology. Materials Today: Proceedings, 43, 28–35.

[24] Petkovic, D., Nikolic, V., Milovancevic, M., and Lazov, L. (2016) Estimation of the most influential factors on the laser cutting process heat affected zone (HAZ) by adaptive neuro-fuzzy technique. Infrared Physics & Technology, 77, 12–15.

[25] Rao, K. V., Raju, L. S., Suresh, G., Ranganayakulu, J., and Krishna, J. (2023) Modelling of kerf width and surface roughness using vibration signals in laser beam machining of stainless-steel using design of experiments. Optics & Laser Technology, 169, 110146.

[26] Rohman, M. N., Ho, J., Tung, P., Lin, C., and Lin, C. (2022) Prediction and optimization of dross formation in laser cutting of electrical steel sheet in different environments. Journal of Materials Research and Technology, 18, 1977–1990.

[27] Sargar, T., Jadhav, A., and Gautam, N. K. (2023) Comparative study of process parameters on dross properties by laser machining of AISI 316L material. Materials Today: Proceedings.

[28] Singh, A. K., Bal, K. S., Pal, A. R., Dey, D., and Choudhury, A. R. (2021) A novel method to reduce dross in laser beam cutting of Ti-6Al-4 V alloy sheet. Journal of Manufacturing Processes, 64, 95–112.

[29] Teixidor, D., Ciurana, J., and Rodriguez, C. A. (2014) Dross formation and process parameters analysis of fibre laser cutting of stainless-steel thin sheets. The International Journal of Advanced Manufacturing Technology, 71 (9–12), 1611–1621.

[30] Sargar, T., Jadhav, A., and Gautam, N. K. (2024) Experimental study of heat affected zone for CO_2 and fiber laser machining of SS 316L material. Materials Today: Proceedings.

[31] Yagi, A., Kadonaga, S., Okamoto, Y., Ishiguro, H., Ito, R., Sugiyama, A., Okawa, H., Fujita, R., and Okada, A. (2020) Fundamental study on reduction of dross in fiber laser cutting of steel by shifting nozzle axis. Journal of Laser Applications, 33 (1).